JACS
JOURNAL OF THE AMERICAN CHEMICAL SOCIETY
Article
pubs.acs.org/JACS

$[MoO(S_2)_2L]^{1-}$ (L = picolinate or pyrimidine-2-carboxylate) Complexes as MoS_x-Inspired Electrocatalysts for Hydrogen Production in Aqueous Solution

Benjamin R. Garrett, Kevin A. Click, Christopher B. Durr, Christopher M. Hadad, and Yiying Wu*

Department of Chemistry and Biochemistry, The Ohio State University, 100 West 18th Avenue, Columbus, Ohio 43210, United States

Supporting Information

ABSTRACT: Crystalline and amorphous molybdenum sulfide (Mo−S) catalysts are leaders as earth-abundant materials for electrocatalytic hydrogen production. The development of a molecular motif inspired by the Mo−S catalytic materials and their active sites is of interest, as molecular species possess a great degree of tunable electronic properties. Furthermore, these molecular mimics may be important for providing mechanistic insights toward the hydrogen evolution reaction (HER) with Mo−S electrocatalysts. Herein is presented two water-soluble Mo−S complexes based around the $[MoO(S_2)_2L_2]^{1-}$ motif. We present ^{1}H NMR spectra that reveal $(NEt_4)[MoO(S_2)_2$picolinate] (Mo-pic) is stable in a d_6-DMSO solution after heating at 100 °C, in air, revealing unprecedented thermal and aerobic stability of the homogeneous electrocatalyst. Both Mo-pic and $(NEt_4)[MoO(S_2)_2$pyrimidine-2-carboxylate] (Mo-pym) are shown to be homogeneous electrocatalysts for the HER. The TOF of 27−34 s^{-1} and 42−48 s^{-1} for Mo-pic and Mo-pym and onset potentials of 240 mV and 175 mV for Mo-pic and Mo-pym, respectively, reveal these complexes as promising electrocatalysts for the HER.

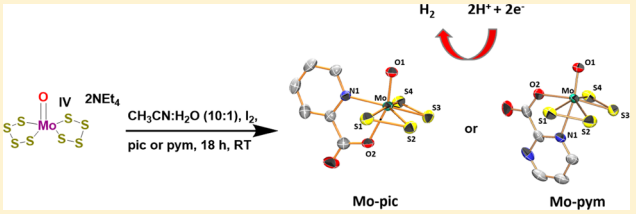

INTRODUCTION

Recent advances have revealed that transition metal chalcogenides, most notably MoS_x (x = 2 to 3), are promising and inexpensive alternatives to Pt for electrochemical generation of H_2 from water.[1−7] Crystalline MoS_2 (c-MoS_2) materials have led to great improvements in earth-abundant catalysts for the HER. Catalytic activity of crystalline MoS_2 materials is thought to be localized to edge sites where disulfide linkages or triangular MoS_2 units are exposed, which has inspired molecular mimics of the edge structures for maximizing the density of catalytic sites.[5−7] The Mo−S cluster complexes $[Mo_3S_4]^{4+}$, $[Mo_3S_{13}]^{2-}$, and $[Mo_2S_{12}]^{2-}$ have been shown to exhibit excellent catalytic activities for heterogeneous catalysis.[5,6,8]

Recently, amorphous MoS_x (a-MoS_x) has been shown to be a scalable material that exhibits activity higher than that of c-MoS_2.[7,9,10] Tran et al. reported that a-MoS_x consists of a polymer of $[Mo_3S_{13}]^{2-}$ repeating units, which indicates that the molecular clusters can be used as building blocks for constructing catalytic materials.[7] Therefore, the Mo−S cluster complexes $[Mo_3S_4]^{4+}$, $[Mo_3S_{13}]^{2-}$, and $[Mo_2S_{12}]^{2-}$ may become even more important when exploring the high catalytic activity of a-MoS_x.

The catalytic mechanism of c-MoS_2 is still under debate, where various studies have evoked different pathways.[11,12] Even less is known about the operating mechanism of the superior catalytic material a-MoS_x. Homogenous catalysts are suited for mechanistic studies because in situ spectroscopic techniques such as NMR, UV−vis, or IR may be conducted to elicit structural information. The complexes $[PY5Me_2MoS_2]^{2+}$ and $MoO(S_2)_2$bpyR have been proposed as molecular electrocatalysts that were inspired by active sites within the catalytic materials.[13,14]

We recently reported on the heptacoordinate molybdenum complexes $MoO(S_2)_2$bpyR (bpyR = 2,2′-bipyrdine (bpy), 4,4′-di-*tert*-butyl-2,2′-bipyrdine (bpy-*tert*-butyl), 4,4′-dimethoxy-2,2′-bipyrdine (bpy-OMe), Mo-bpy), where the catalytic performance of the series of complexes could be tuned by varying the functional group on the bpy ligand. Interestingly, in the recent report on a-MoS_x composed of polymeric $[Mo_3S_{13}]^2$, in situ Raman spectroscopy revealed the presence of a Mo═O moiety during catalytic cycling (Figure 1a). Furthermore, after

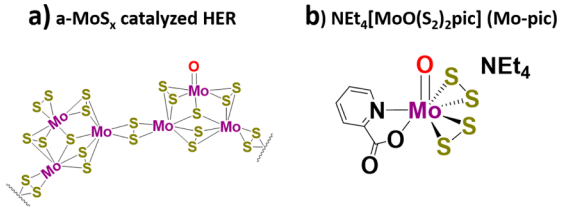

Figure 1. Recent reports revealed the participation of a Mo═O moiety in the active site of a-MoS_x. The molecular homogeneous electrocatalyst Mo-pic may serve as a mimic for the active sites in a-MoS_x.

Received: August 18, 2016
Published: October 3, 2016

DOI: 10.1021/jacs.6b08652
J. Am. Chem. Soc. 2016, 138, 13726−13731

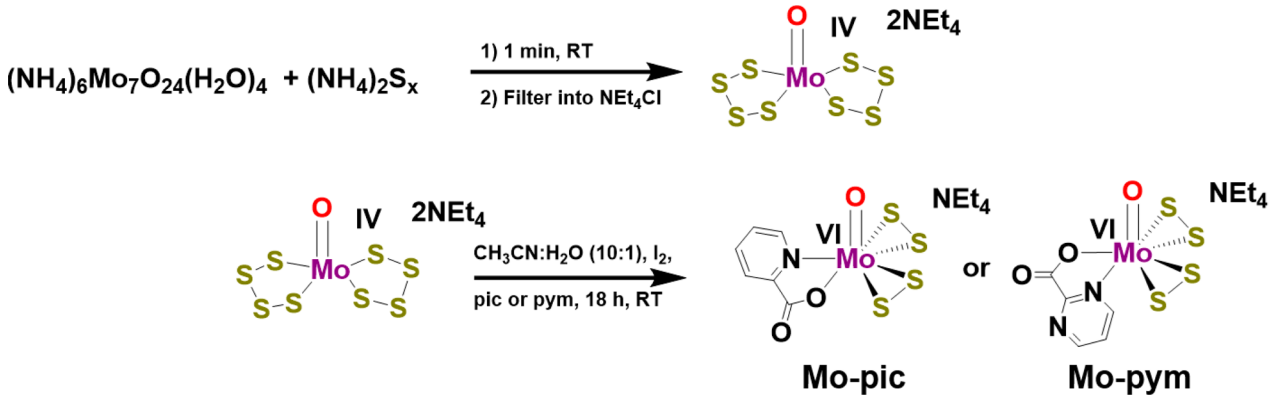

Figure 2. Complexes Mo-pic and Mo-pym were synthesized through a novel synthetic route, where $(NEt_4)_2[MoO(S_4)_2]$ is oxidized with I_2 to afford the precursor (Figure S1), which reacts with the bidendate ligands picolinic acid (pic) or pyrimidine-2-carboxylic acid (pym) to form the products Mo-pic and Mo-pym.

dissolving the catalytic a-MoS_x in HNO_3 and conducting elemental analysis, it was revealed that the main composition is MoS_4X, where X accounted for anywhere from 5% to 15% by weight and was determined to be oxygen. Thus, the catalytic moiety in a-MoS_x may share composition with our $[MoO(S_2)_2L_2]^{1-}$ (Mo = 40%, S = 53%, O = 7% by weight) catalytic moiety[14] (Figure 1b).

The new family of picolinate-based catalysts, Mo-pic and Mo-pym, presented herein expands the family of the catalytic $MoO(S_2)_2L_2$ motif, providing water-soluble derivatives. Herein we demonstrate a new synthetic route leading to the ability to tune catalytic properties of a water-soluble family of the $MoO(S_2)_2L_2$ motif. The TOF of 27−34 s^{-1} and 42−48 s^{-1} and onset potentials of 240 mV and 175 mV for Mo-pic and Mo-pym, respectively, reveal these complexes as promising electrocatalysts for the HER. We believe the water-soluble complexes presented herein may prove to be molecular models for some of the most catalytically active earth-abundant materials for the HER, a-MoS_x.

RESULTS AND DISCUSSION

Synthesis. The utility of the heptacoordinate Mo−S complexes for electrocatalytic hydrogen production bearing tunable bpy ligands was recently reported.[14] Previously, a new synthetic method was introduced whereby the thiophilicity of Mo was utilized by exposing peroxo (O_2^{2-}) complexes of the form $MoO(O_2)_2$bpyR to an ammonium polysulfide solution. In a review published by Conte and Floris in 2011, greater than 30 various Mo complexes bearing the $MoO(O_2)_2L_2$ moeity are reported.[15] It was the large family of peroxo complexes that led to our excitement about the persulfide (S_2^{2-}) ligand exchange procedure, which produced $MoO(S_2)_2$bpyR from the well-studied $MoO(O_2)_2$bpyR.

The three catalysts previously reported all contain bpy derivatives as the ligand (L) in $MoO(S_2)_2L_2$. As our interest lies in developing the $MoO(S_2)_2L_2$ complexes as tunable water reduction catalysts, it is desirable to conduct homogeneous electrocatalysis in aqueous conditions, as water is a much more attractive medium for the sustainable generation of hydrogen.[16] The neutral Mo-bpy complexes were insoluble in aqueous solutions and even mixed solvent systems. Therefore, using the large library of the $MoO(O_2)_2L_2$ complexes, we sought ionic derivatives that would thereby impart water solubility.[15]

We began our efforts focused on picolinate derivatives which would give the anionic complex $[MoO(S_2)_2pic]^-$ (pic = picolinate). Isolation and purification of $[MoO(S_2)_2pic]^-$ from $[MoO(O_2)_2pic]^-$ proved troublesome for the water-soluble complexes using the previously reported route.[14] Besides our work, the number of examples of Mo complexes containing the $MoO(S_2)_2$ moeity is limited.[17−20] In 1999, Coucouvanis suggested in a review on Mo−S cluster chemistry that the $(NEt_4)[Mo_2O_2S_8Cl]$ dimer may be a precursor for synthesis of $MoO(S_2)_2L_2$ species.[21] Steps 1−3 in Figure S1 have therefore been reported, but the final step of making $MoO(S_2)_2L_2$ species from $(NEt_4)[Mo_2O_2S_8Cl]$ has not.[22]

Inspired by the work on $(NEt_4)[Mo_2O_2S_8Cl]$, the monomer $(NEt_4)_2[MoO(S_4)_2]$ was synthesized according to the literature procedure in up to a 30 g scale.[22] The monomer was then oxidized with iodine to form an intermediate, which is suited for addition of bidentate ligands.[21,22] We found that for picolinic acid (pic) and pyramidine-2-carboxyic acid (pym), the addition of I_2 to an acetonitrile slurry of $(NEt_4)_2[MoO(S_4)_2]$, in the presence of pic or pym afforded $(NEt_4)[MoO(S_2)_2pic]$ (Mo-pic) and $(NEt_4)[MoO(S_2)_2pym]$ (Mo-pym) as a reddish/purple powder in 76−84% yields. The unique one-pot synthesis of $[MoO(S_2)_2L_2]^{1-}$ moieties is a mild, modular method to produce many interesting complexes. The two Mo−S material-inspired complexes were synthesized open to air, in two steps from low-cost materials, thus illustrating their potential for scalability. Figure 2 outlines the synthetic pathway developed and used for the synthesis of the two complexes presented.

Characterization. Single crystals were grown by slow evaporation of acetonitrile:toluene (1:1) solvent mixtures, and structure determinations were carried out on Mo-pic and Mo-pym. Both anionic complexes are similar in structure to previously reported heptacoordinate mononuclear Mo−S complexes, and structures of the anions are presented in Figure 3 (Figure S3 includes the full crystal structure).[14,19,23] It is noteworthy that pym exhibits binding to the Mo center different from that of pic. The coordinating oxygen and nitrogen in pym binds in the equatorial and axial position, respectively. When pic was used as the ligand, the coordinating oxygen and nitrogen bind in the axial and equatorial position, respectively. The difference in binding between the ligands affects bonding distances. The Mo−N1 equatorial bonding distances in pic is 2.218 Å, whereas the Mo−O1 equatorial bonding distance in pym (2.097 Å) is significantly shorter. A table of select bond distances is presented in Table S1.

The ^1H NMR spectrum of Mo-pic and Mo-pym in deuterated acetonitrile (CD_3CN) exhibit two sets of peaks,

DOI: 10.1021/jacs.6b08652
J. Am. Chem. Soc. 2016, 138, 13726−13731

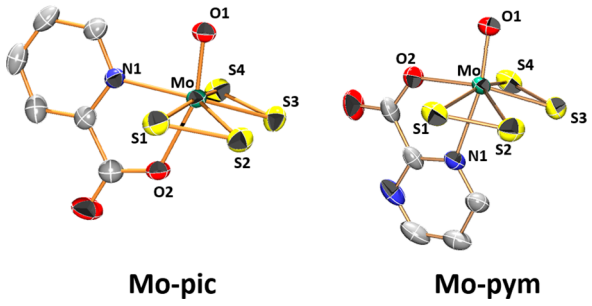

Figure 3. X-ray crystal structures of the anion of Mo-pic and Mo-pym illustrating the different binding modes of the N,O bidentate ligands presented in this work. Thermal ellipsoids are shown at 50% probability, and hydrogen atoms are omitted for clarity. A full structure, including the NEt_4^+ counterion, is presented in Figure S3.

both identified as Mo-pic and Mo-pym where the nitrogen in pic and pym may bind in either equatorial or axial position (Figure 4). Figures S6–S9 present ^{1}H NMR spectra of pic and Mo-pic, and pym and Mo-pym, illustrating that the second set of peaks is not due to uncoordinated ligand. The Gibbs free energy, as calculated by determining K_{eq} by integrating the doublets at 9.30 and 7.92 ppm, was determined to be −0.56 kcal/mol for Mo-pic and 0.34 kcal/mol for Mo-pym (doublets at 9.52 and 8.78 ppm used for Mo-pym) in acetonitrile (Figure 4). Variable temperature ^{1}H NMR in d_6-dimethyl sulfoxide (d_6-DMSO) was conducted up to 95 °C, and no coalescence of peaks was found (Figure S11). d_6-DMSO was used in the VT-NMR experiment in order to reach higher temperatures. The low Gibbs free energy difference and the lack of coalescence of peaks at high temperature in the VT-NMR experiment indicate a small difference thermodynamically between the two conformations. It is worth noting that the ^{1}H NMR spectrum of Mo-pic after cooling back to 27 °C (after heating up to 95 °C in air) remains unchanged (Figure S12). To our knowledge, this kind of stability is unprecedented for homogeneous molecular electrocatalysts.

Understanding the major conformation in catalytic conditions is important. When the nitrogen in pic or pym is bound in the equatorial position (eq), the closer bond distance is thought to contribute to stronger deshielding, resulting in an upfield shift in the peak position of the aromatic protons. From the relative upfield shift in the ^{1}H NMR spectrum, we are able to deduce the major conformation in various solvent systems. Catalytic experiments, as discussed below, were conducted in a pH 3 buffer/acetonitrile mixed solution. The ^{1}H NMR spectrum of Mo-pic in a D_2O:CD_3CN (6:4) solution showed only one confirmation. On the basis of the higher field shifts of the aromatic peaks of Mo-pic in the D_2O:CD_3CN solution, the Mo-pic is thought to be in the conformation where the nitrogen in pic is in the equatorial position. The ^{1}H NMR spectrum of Mo-pym in a D_2O:CD_3CN (6:4) solution showed two confirmations present. On the basis of the higher field shifts of the aromatic peaks of Mo-pym in the D_2O:CD_3CN solution, the major Mo-pym is thought to consist of the conformation where the nitrogen in pym is in the equatorial position. Therefore, the major conformation of Mo-pym differs depending on the makeup of the solvent.

It is noteworthy that pic does not exhibit the ligand flunctionality that pym shows in the D_2O:CD_3CN solvent mixtures. The difference may be explained in the binding ability of the coordinating nitrogen in pic and pym, which may be

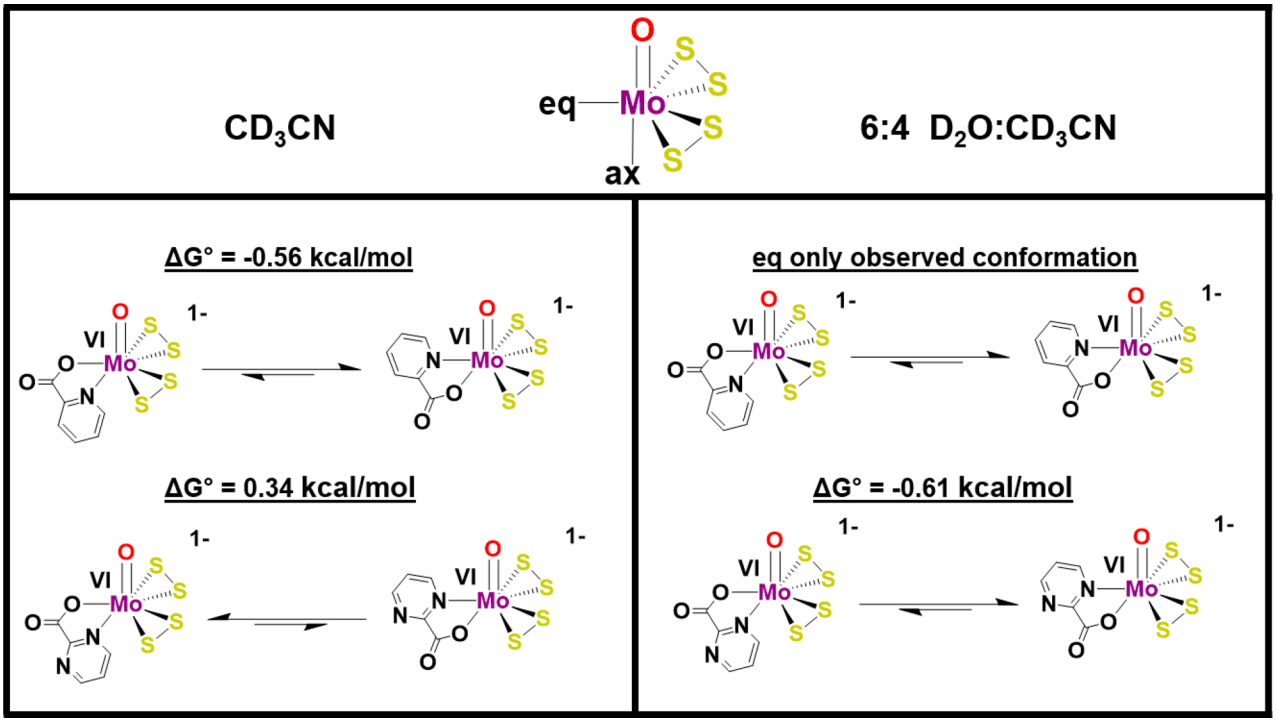

Figure 4. Understanding the major confirmation in Mo-pic and Mo-pym in catalytic conditions is important for elucidating information about catalyst performance. Either pic or pym may bind where the nitrogen is equatorial (eq) or axial (ax). The bound nitrogen has a shorter bond distance when in the eq position. The closer interaction with the electron-deficient Mo center deshields the protons in the aromatic ring, allowing the distinction between the two conformations in solution. Equilibrium arrows are presented, indicating the favored configuration in the deuterated solvents tested.

DOI: 10.1021/jacs.6b08652
J. Am. Chem. Soc. 2016, 138, 13726–13731

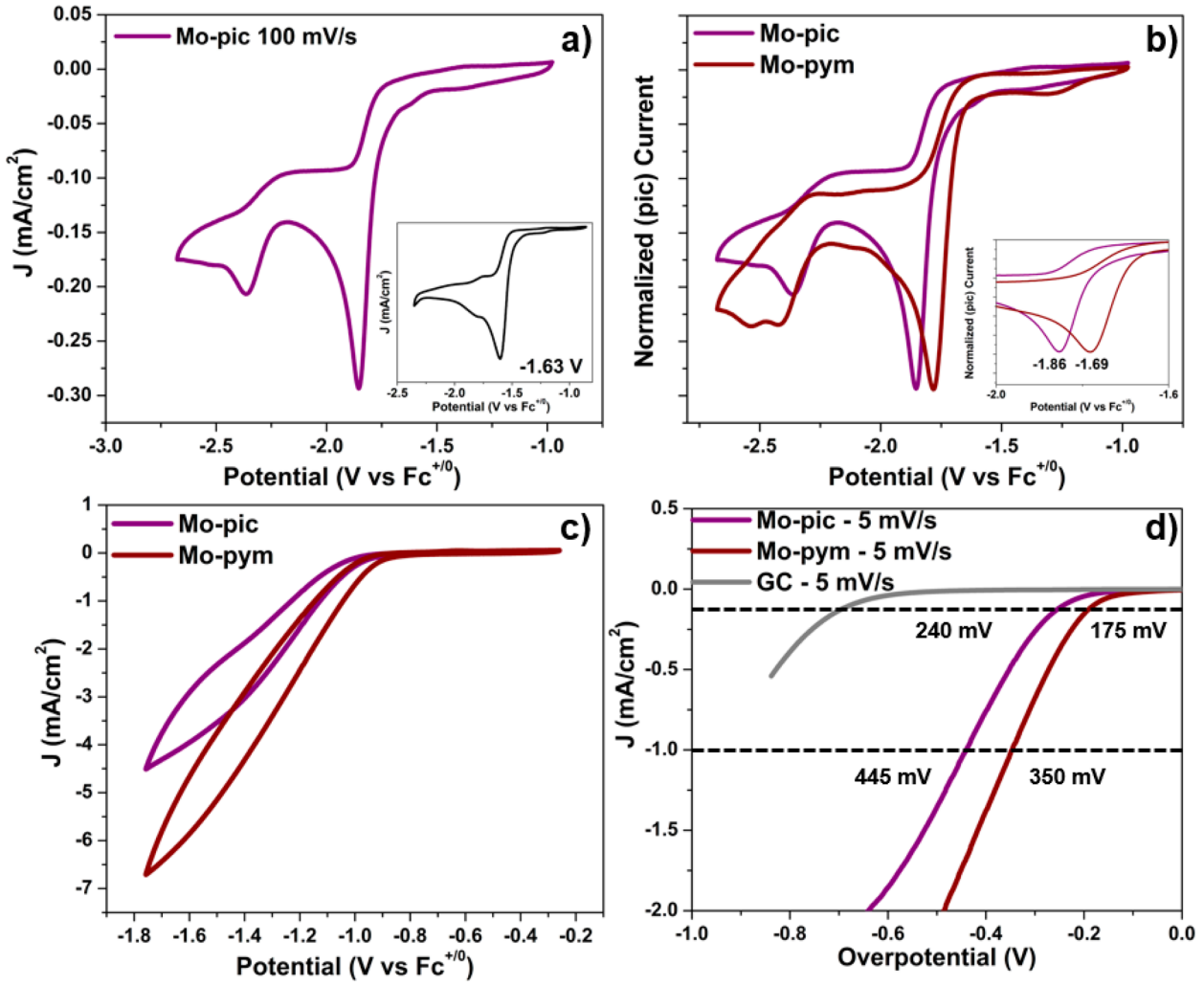

Figure 5. (a) A CV of a 2 mM solution of Mo-pic in acetronitrile with 0.1 M $TBAPF_6$ as supporting electrolyte is presented. An inlay of a CV of Mo-bpy is presented under similar conditions, illustrating the similarities in the reductive peaks. (b) CVs of both Mo-pic and Mo-pym are presented, showing similar reductive processes between the two derivatives. An inlay demonstrates the tunability in an acetonitrile solution of the reduction of the two species. (c) CVs of both Mo-pic and Mo-pym are presented in a pH 3 citrate buffer and acetronitrile mixed solvent system (6:4), showing an increase in cathodic current, indicative of catalytic proton reduction. (d) LSVs of Mo-pic and Mo-pym are presented. A detailed discussion on how overpotential is determined is included in the main text. Both Mo−S derivatives presented in this work illustrate excellent overpotentials for hydrogen evolution.

related to pK_as of the protonated forms. For example, the pK_a of pyridinium is reported to be 5.2, whereas the pK_a of pyrimidinium is reported to be 1.3. Thus, the extra nitrogen in the aromatic ring greatly effects the binding nature of the nitrogen in pym relative to pic. The fluxionality of the ligands we report may be important for future mechanistic investigations.

Electrochemistry. All cyclic voltammograms (CVs) and linear sweeps voltammograms (LSVs) are reported versus an internal ferrocene ($Fc^{+/0}$) standard unless otherwise noted. The reduction of heptacoordinate molybdenum chalcogenides have been explored by theory and experiment.[14,24] Both of the reports reveal cyclic voltammagrams with two irreversible reduction peaks and suggest the participation of the chalcogenide ligand in the redox processes. The CV of $MoO(S_2)_2$bpy revealed an irreversible reduction peak followed by another reduction peak at a slightly more negative potential. Given the more donating character of pic relative to bpy, one would expect a negative shift in reduction potential of Mo-pic relative to Mo-bpy. Figure 5a presents the CV of a 2 mM solution of Mo-pic in acetonitrile, with a 0.1 M tetrabutylammonium hexafluorophosphate ($TBAPF_6$) supporting electrolyte, glassy carbon working electrode (GC WE), $Ag/AgNO_3$ reference electrode, and graphite rod counter electrode. A CV of Mo-bpy using similar conditions (*N*,*N*′-dimethylformamide (DMF) was used as the solvent rather than CH_3CN) is presented as an inset. The first reduction potential of Mo-pic was 230 mV more negative than that of Mo-bpy (−1.86 V, and −1.63 V vs $Fc^{+/0}$). One would expect the reduction of Mo-pym to be more positive than that of Mo-pic due to the additional nitrogen in the aromatic ring of pym relative to pic. A CV of both Mo-pic and Mo-pym is presented in Figure 5b indicating the more positive onset in reduction potential, thus illustrating the tunability of the new $[MoO(S_2)_2L_2]^{1-}$ moieties.

An aqueous solvent system was needed that was acidic and in which Mo-pic and Mo-pym were soluble and stable. UV−vis spectra of Mo-pic and Mo-pym in a 6:4 pH 3 citric acid buffer:acetonitrile solution are presented in Figure S12. Additionally, the adsorption at 545 nm was also monitored, revealing the stability of the catalyst over 1 h in the catalytic

DOI: 10.1021/jacs.6b08652
J. Am. Chem. Soc. 2016, 138, 13726−13731

conditions. A CV of Mo-pic and Mo-pym in a 6:4 pH 3 citric acid buffer:acetonitrile solution is presented in Figure 5c, revealing an increase in cathodic current relative to acetonitrile solutions. The increase in cathodic current is the first indication of catalysis for hydrogen production.

It was previously shown that when recording a CV of $[MoS_4]^{2-}$ one oxidation and one reduction peak grows in at −0.1 V and −0.6 V vs SHE, respectively, indicating the formation of a-MoS_x films on the working electrode.[9] Figures S13 and S14 present CVs of Mo-pic and Mo-pym over multiple cycles in a similar potential window as for a-MoS_x formation, showing no indicative a-MoS_x peaks. Furthermore, LSVs of a fresh 6:4 pH 3 citric acid buffer:acetonitrile solution with the unpolished WE used in the LSV for Mo-pic and Mo-pym experiments revealed that no catalytic deposits on the GC WE were apparent. GC-MS of headspace over 1 h revealed hydrogen was indeed produced with a TOF of 27−34 s^{-1} and 42−48 s^{-1} for Mo-pic and Mo-pym. Figures S16 and S17 detail how TOFs were calculated for each derivative. Faradaic efficiencies after 1 h of controlled potential electrolysis at 540 mV overpotential were calculated to be 40−49% for Mo-pic and 75−78% for Mo-pym. The discrepancy in faradaic efficiencies between the two similar derivatives may be due to the ligand fluxionality in the catalytic solvent, as discussed above (Figure 4). Current efforts are underway to investigate the mechanism of the catalysts presented and how the ligand fluxionality in solution affects catalysis.

The overpotential for hydrogen production is an equally important metric for comparing catalytic performance of homogeneous catlaysts as TOF. Recent reports have revealed that measuring the open circuit potential (OCP) of the catalytic system of interest is among the best methods to report overpotentials.[25−28] The method is especially useful in providing consistency in determining overpotentials in mixed solvent systems. The overpotential vs $Fc^{+/0}$ of the HER in a 6:4 pH 3 citric acid buffer:acetonitrile solution with a saturated H_2 atmosphere was determined to be 760 mV as determined by measuring the OCP between a Pt mesh and $Ag/AgNO_3$ RE (referenced vs an internal $Fc^{+/0}$ standard). Linear sweep voltammograms (LSV) of Mo-pic and Mo-pym presented in Figure 5d (dashed line) reveal an onset potential of 240 mV and 175 mV for Mo-pic and Mo-pym. Furthermore, overpotentials at −1 mA/cm^2 were 445 mV and 350 mV for Mo-pic and Mo-pym.

The overpotentials presented in this work place their activities for the HER among some of the best polypyridyl homogeneous electrocatalysts. For example, the $[PY5Me_2MoO]^{2+}$ and $[PY5Me_2MoS_2]^{2+}$ complexes, at an overpotential of 0.99 and 0.78 V, respectively, display a TOF of 2.4 s^{-1} and 230 s^{-1}.[13,29,30] Mo-pic and Mo-pym presented herein, at an overpotential of 0.54 V, displayed a TOF of 27−34 s^{-1} and 42−48 s^{-1}. Additionally, the ligands used in this work, pic and pym, are commercially available (pic = $0.47/g from Sigma-Aldrich, pym = $7.90/g from Matrix Scientific) compared to the more complex polypyridyl ligands used in previous work.[30]

CONCLUSION

Crystalline and amorphous molybdenum sulfide materials have been leading materials for catalytic hydrogen production using earth-abundant materials. The molybdenum sulfide materials have inspired the synthesis of the homogeneous electrocatalysts Mo-pic and Mo-pym using a new, mild synthetic route. The new complexes exhibit electrochemical behavior similar to that of our previous complexes and illustrate tunability in addition to being soluble in aqueous solutions. The overpotentials and TOF of Mo-pic and Mo-pym reveal these complexes as promising homogeneous electrocatalysts for hydrogen production. Further optimization of catalyst performance by ligand tuning is underway in our group. Furthermore, the role of ligand fluxionality presented in this work is being explored for its importance in catalyst performance.

EXPERIMENTAL SECTION

General Considerations. All reactions and operations were carried out open to air, in a well ventilated hood. All commercially available reagents were of ACS grade and used without further purification. ^{1}H NMR spectra were recorded on a 400 MHz Bruker spectrometer and are reported relative to TMS. High-resolution mass spectra were obtained on Bruker MicroTOF mass spectrometer from the mass spectrometry facility at The Ohio State University. Solid-state IR spectra were recorded using a PerkinElmer FTIR/MidIR spectrometer. Cyclic voltammetry measurements were performed using a Gamry Reference 600 potentiostat. All voltammograms were obtained in a three-electrode cell under Ar atmosphere at room temperature. The working electrode was a glassy carbon disk (0.071 cm^2), and a graphite rod was used as the auxiliary electrode. The experimental reference electrode was $Ag/AgNO_3$, and measured potentials are reported vs $Fc^{+/0}$ as determined from recording with an internal reference of Cp_2Fe/Cp_2Fe^+.[31] Hydrogen was detected using a Shimadzu gas chromatograph equipped with a thermal conductance detector using argon as the carrier gas. The instrument was calibrated by injecting known volumes of hydrogen (Figure S18).

X-ray Structure Determination. Details of X-ray structure determination and crystallographic data are summarized in the Supporting Information.

$(NEt_4)_2[MoO(S_4)_2]$. Bis(tetraethylammonium) bis(tetrasulfido)-oxomolybdate(IV) was synthesized as previously reported.[22] Yield: 31 g (87%). FT-IR (ATR): 926, 781, 514 cm^{-1}

Synthesis of $NEt_4[MoO(S_2)_2pic]$ and $NEt_4[MoO(S_2)_2pym]$ (Mo-pic and Mo-pym). To a 50 mL round-bottom flask equipped with a stir bar were added $(NEt_4)_2[MoO(S_4)_2]$ (1 g, 1.6 mmol), I_2 (200 mg, 0.8 mmol), picolinic acid or pyrimidine-2-carboyxlic acid (0.39 g, 3.2 mmol, 2 equiv (pic) or 0.40 g, 3.2 mmol, 2 equiv (pym)), 1 mL of H_2O, and 10 mL of acetonitrile. The slurry was stirred for 18 h, turning from a dark red slurry to a dark purple solution. The solution was filtered, removing S_8 and NEt_4I. Solvent was removed from the filtrate, affording a dark red/purple solid. The solid was then washed with two 10 mL portions of ice-cold water and dried in vacuo for 1 h.

$NEt_4[MoO(S_2)_2pic]$. Yield: 0.60 g (76%). FT-IR (ATR): 1659, 919, 535 cm^{-1}; ESI-MS: m/z 363.813 $[M^-]$; UV−vis [6:4 pH 3 citric acid buffer:acetonitrile; $\lambda_{abs,max}$ (nm)/ε (M^{-1} cm^{-1})]: 480/1033, 550/1097. ^{1}H NMR (400 MHz, 6:4 D_2O:CD_3CN): δ 9.28 (d, 1H, J = 5.36 Hz), 8.38 (td, 1H, J = 1.43 Hz), 8.14 (d, 1H, J = 7.72 Hz), 7.96 (m, 1H), 3.11 (q, 8H, J = 7.29 Hz), 1.14 (m, 12H)

$NEt_4[MoO(S_2)_2pym]$. Yield: 0.64 g (82%). FT-IR (ATR): 1661, 922, 538 cm^{-1}; ESI-MS: m/z 364.809 $[M^-]$; UV−vis [6:4 pH 3 citric acid buffer:acetonitrile; $\lambda_{abs,max}$ (nm)/ε (M^{-1} cm^{-1})]: 480/1236, 545/1277. ^{1}H NMR of major conformation (400 MHz, 6:4 D_2O:CD_3CN): δ 9.52 (dd, 1H, J = 2.02 Hz), 9.27 (dd, 1H, 2.02 Hz), 8.03 (t, 1H, 5.25), 3.11 (q, 8H, J = 7.29 Hz), 1.14 (m, 12H).

ASSOCIATED CONTENT

Supporting Information

The Supporting Information is available free of charge on the ACS Publications website at DOI: 10.1021/jacs.6b08652.

UV−vis, FTIR, and ^{1}H NMR spectra. Cyclic voltammetry data (PDF)
X-ray crystallographic data (PDF)
CIF data for Mo-pic (CIF)

DOI: 10.1021/jacs.6b08652
J. Am. Chem. Soc. 2016, 138, 13726−13731

CIF data for Mo-pym (CIF)

AUTHOR INFORMATION

Corresponding Author

*wu.531@osu.edu

Notes

The authors declare no competing financial interest.

CCDC 1499761 and CCDC 1499762 contain the supplementary crystallographic data for complexes Mo-pic and Mo-pym. These data can be obtained free of charge via http://www.ccdc.cam.ac.uk/conts/retrieving.html or from the Cambridge Crystallographic Data Centre, 12 Union Road, Cambridge CB2 1EZ, UK; fax: (+44) 1223-336-033; or e-mail: deposit@ccdc.cam.ac.uk.

ACKNOWLEDGMENTS

We acknowledge exceptional support and discussion from William McCulloch, Thomas Draskovic, Ryan McKenney, and Maneesha Pimplikar. We thank Professor Scott Bunge for assistance in collecting crystallographic data. We also thank Suzanne Witt and Professor Turro for the use of their GC-TCD. We acknowledge support from the NSF Chemistry Catalysis Program of the Chemistry Division − CHE-1566106.

REFERENCES

(1) Jaramillo, T. F.; Jørgensen, K. P.; Bonde, J.; Nielsen, J. H.; Horch, S.; Chorkendorff, I. *Science* **2007**, *317*, 100−102.

(2) Laursen, A. B.; Kegnæs, S.; Dahl, S.; Chorkendorff, I. *Energy Environ. Sci.* **2012**, *5*, 5577−5591.

(3) Gao, M. R.; Xu, Y. F.; Jiang, J.; Yu, S. H. *Chem. Soc. Rev.* **2013**, *42*, 2986−3017.

(4) Chhowalla, M.; Shin, H. S.; Eda, G.; Li, L. J.; Loh, K. P.; Zhang, H. *Nat. Chem.* **2013**, *5*, 263−275.

(5) Kibsgaard, J.; Jaramillo, T. F.; Besenbacher, F. *Nat. Chem.* **2014**, *6*, 248−253.

(6) Huang, Z.; Luo, W.; Ma, L.; Yu, M.; Ren, X.; He, M.; Polen, S.; Click, K.; Garrett, B.; Lu, J.; Amine, K.; Hadad, C.; Chen, W.; Asthagiri, A.; Wu, Y. *Angew. Chem., Int. Ed.* **2015**, *54*, 15181−15185.

(7) Tran, P. D.; Tran, T. V.; Orio, M.; Torelli, S.; Truong, Q. D.; Nayuki, K.; Sasaki, Y.; Chiam, S. Y.; Yi, R.; Honma, I.; Barber, J.; Artero, V. *Nat. Mater.* **2016**, *15*, 640−646.

(8) Jaramillo, T. F.; Bonde, J.; Zhang, J.; Ooi, B. L.; Andersson, K.; Ulstrup, J.; Chorkendorff, I. *J. Phys. Chem. C* **2008**, *112*, 17492−17498.

(9) Merki, D.; Fierro, S.; Vrubel, H.; Hu, X. *Chem. Sci.* **2011**, *2*, 1262.

(10) Benck, J. D.; Chen, Z.; Kuritzky, L. Y.; Forman, A. J.; Jaramillo, T. F. *ACS Catal.* **2012**, *2*, 1916−1923.

(11) Huang, Y.; Nielsen, R. J.; Goddard, W. A.; Soriaga, M. P. *J. Am. Chem. Soc.* **2015**, *137*, 6692−6699.

(12) Lassalle-kaiser, B.; Merki, D.; Vrubel, H.; Gul, S.; Yachandra, V. K.; Hu, X.; Yano, J.; Merisiers, L. O. *J. Am. Chem. Soc.* **2015**, *137*, 314−321.

(13) Karunadasa, H. I.; Montalvo, E.; Sun, Y.; Majda, M.; Long, J. R.; Chang, C. J. *Science* **2012**, *335*, 698−702.

(14) Garrett, B. R.; Polen, S. M.; Click, K. A.; He, M.; Huang, Z.; Hadad, C. M.; Wu, Y. *Inorg. Chem.* **2016**, *55*, 3960−3966.

(15) Conte, V.; Floris, B. *Dalton Trans.* **2011**, *40*, 1419−1436.

(16) Cook, T. R.; Dogutan, D. K.; Reece, S. Y.; Surendranath, Y.; Teets, T. S.; Nocera, D. G. *Chem. Rev.* **2010**, *110*, 6474−6502.

(17) Mennemann, K.; Mattes, R. *Angew. Chem., Int. Ed. Engl.* **1977**, *16*, 260−261.

(18) Leonard, K.; Plute, K.; Haltiwanger, R. C.; DuBois, M. R. *Inorg. Chem.* **1979**, *18*, 3246−3251.

(19) Chakrabarty, P. K.; Bhattacharya, S.; Pierpont, C. G.; Bhattacharyya, R. *Inorg. Chem.* **1992**, *31*, 3573−3577.

(20) Gushchin, A. L.; Laricheva, Y. L.; Alferova, N. I.; Virovets, A. V.; Sokolov, M. N. *J. Struct. Chem.* **2013**, *54*, 752−758.

(21) Coucouvanis, D. *Adv. Inorg. Chem.* **1998**, *45*, 1−73.

(22) Hadjikyriacou, A. I.; Coucouvanis, D. *Inorg. Chem.* **1989**, *28*, 2169−2177.

(23) McConnachie, C. A.; Stiefel, E. I. *Inorg. Chem.* **1999**, *38*, 964−972.

(24) Bonchio, M.; Conte, F.; Di Furia, F.; Modena, G.; Moro, S.; Carofiglio, T.; Magno, F.; Pastore, P. *Inorg. Chem.* **1993**, *32*, 5797−5799.

(25) Pool, D. H.; Stewart, M. P.; Hagan, M. O.; Shaw, W. J.; Roberts, J. A. S.; Bullock, R. M.; DuBois, D. L.; O'Hagan, M. *Proc. Natl. Acad. Sci. U. S. A.* **2012**, *109*, 15634−15639.

(26) Appel, A. M.; Helm, M. L. *ACS Catal.* **2014**, *4*, 630−633.

(27) Roberts, J. A. S.; Bullock, R. M. *Inorg. Chem.* **2013**, *52*, 3823−3835.

(28) Rountree, E. S.; McCarthy, B. D.; Eisenhart, T. T.; Dempsey, J. L. *Inorg. Chem.* **2014**, *53*, 9983−10002.

(29) Karunadasa, H. I.; Chang, C. J.; Long, J. R. *Nature* **2010**, *464*, 1329−1333.

(30) Zee, D. Z.; Chantarojsiri, T.; Long, J. R.; Chang, C. J. *Acc. Chem. Res.* **2015**, *48*, 2027−2036.

(31) Connelly, N. G.; Geiger, W. E. *Chem. Rev.* **1996**, *96*, 877−910.

DOI: 10.1021/jacs.6b08652
J. Am. Chem. Soc. 2016, 138, 13726−13731